

White-Light Filaments for Atmospheric Analysis

J. Kasparian,^{1*} M. Rodriguez,² G. Méjean,¹ J. Yu,¹ E. Salmon,¹ H. Wille,² R. Bourayou,^{2,3} S. Frey,^{1,2} Y.-B. André,⁴ A. Mysyrowicz,⁴ R. Sauerbrey,³ J.-P. Wolf,¹ L. Wöste²

Most long-path remote spectroscopic studies of the atmosphere rely on ambient light or narrow-band lasers. High-power femtosecond laser pulses have been found to propagate in the atmosphere as dynamically self-guided filaments that emit in a continuum from the ultraviolet to the infrared. This white light exhibits a directional behavior with enhanced backward scattering and was detected from an altitude of more than 20 kilometers. This light source opens the way to white-light and nonlinear light detection and ranging applications for atmospheric trace-gas remote sensing or remote identification of aerosols. Air ionization inside the filaments also opens promising perspectives for laser-induced condensation and lightning control. The mobile femtosecond-terawatt laser system, Teramobile, has been constructed to study these applications.

Remote sensing of the atmosphere is necessary for determining both the chemical and dynamic processes that affect problems such as global warming, ozone loss, tropospheric pollution, and weather prediction. Some approaches bring the instrument to the remote sample, for example, balloon- and aircraft-borne instruments that analyze composition through techniques like mass spectrometry (*1*). The variety of data provided by this type of instrument is difficult to achieve with other methods, but those local methods can be expensive for routine daily studies needed to create archival data sets. The other main approach is to use optical spectrometry to probe a long path through the atmosphere. The path can be fixed, as is the case with Fourier-transform infrared spectroscopy (FTIR) and differential optical absorption spectroscopy (DOAS). These methods allow us to retrieve precise data about the abundance of a large group of atmospheric constituents from the optical absorption of the sunlight or moonlight along its path across the atmosphere (*1*). The light detection and ranging (LIDAR) method, based on atmospheric backscatter signals from actively emitted light pulses, is free from such predetermined absorption

paths and provides three-dimensional distributions of atmospheric trace gases, as well as aerosol abundance, size, and phase information (*1*). LIDAR, however, is generally restricted to the detection of only one substance at a time. For example, in differential absorption LIDAR (DIAL), two lasers are used to monitor trace gases. One emits at the wavelength of peak absorption of the target trace gas, and the other emits at a nearby wavelength where the target gas does not absorb radiation. The difference in the decay between the signals from both lasers will reflect the target gas's concentration.

The main limitation of these long-path absorption methods is that they are constrained by their light sources. Methods that use the Sun or Moon as light sources are path- or intensity-limited, and laser sources are wavelength-limited and hence require multiple instruments for what is essentially the same experiment. Finally, LIDAR is not well suited for the analysis of aerosol compositions such as the identification of bioaerosols.

The need for an atmospheric sensor that combines the advantages of DOAS, FTIR, and LIDAR resulted in the idea of producing a remote “white lamp” by generating a laser-induced plasma focus in the atmosphere. Recent advances in ultrafast lasers have shown that high-power laser light can, under certain power and focusing conditions, create extended regions of ultra-intense illumina-

tion (*2–4*). To reach the required power at the remote location, we designed an experiment to send a slightly focused, high-power femtosecond laser pulse (100 fs, 3 TW) into the atmosphere with an initial negative chirp, that is, with the shorter wavelengths emitted before the longer ones. Instead of a small spot of a plasma focus, an extended white-light channel was observed (*5, 6*) (Fig. 1), similar to previous observations on shorter scales in the laboratory (*2–4*). Unlike the fundamental infrared laser wavelength (~ 800 nm), the white-light channel was clearly visible to the naked eye (*5, 6*). [See the photograph on page 54 of this issue (*4*).] The phenomenon also occurred with a spatially unfocused laser beam. The spectrum of the emitted light covered the entire visible range from the ultraviolet (UV) to the infrared (IR), and its signal could be detected from altitudes beyond 10 km.

The fundamental aspects of the observed nonlinear optical phenomena and their potential application for optical remote sensing (fs LIDAR) provide the basis for the Teramobile

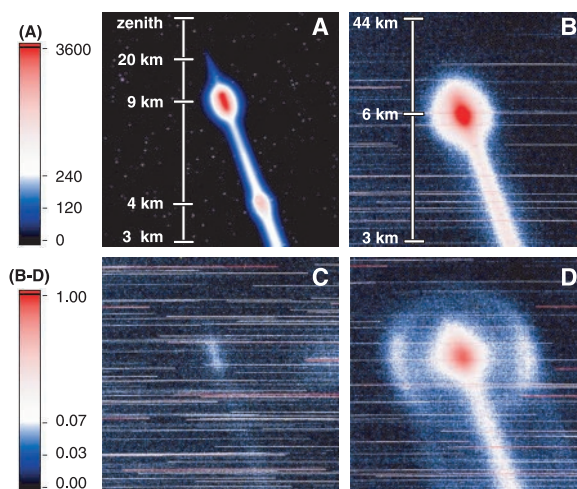


Fig. 1. Long-distance white-light propagation and control of nonlinear optical processes in the atmosphere. Images of the Teramobile fs laser beam propagating vertically were taken with the charge-coupled device camera at TLS observatory. (A) Fundamental wavelength, exhibiting signals from more than 20 km and multiple-scattering halos on haze layers at 4- and 9-km altitudes. (B to D) White light (385 to 485 nm) emitted by the fs laser beam. These images have the same altitude range, and their common color scale is normalized to allow direct comparison with that of (A). (B) With GVD precompensation. (C) Without GVD precompensation. (D) With slight GVD precompensation. The conical emission imaged on a haze layer is apparent.

¹Teramobile project, Laboratoire de Spectrométrie Ionique et Moléculaire, UMR CNRS 5579, Université Claude Bernard Lyon 1, 43 boulevard du 11 novembre 1918, F-69622 Villeurbanne Cedex, France. ²Teramobile project, Institut für Experimentalphysik, Freie Universität Berlin, Arnimallee 14, D-14195 Berlin, Germany. ³Teramobile project, Institut für Optik und Quantenelektronik, Max-Wien-Platz 1, D-07743 Jena, Germany. ⁴Teramobile project, Laboratoire d'Optique Appliquée, UMR CNRS 7639, ENSTA-Ecole Polytechnique, Centre de l'Yvette, Chemin de la Hunière, F-91761 Palaiseau Cedex, France.

*To whom correspondence should be addressed. E-mail: jkaspari@lasim.univ-lyon1.fr

REVIEW

project. Among the main goals of the project are the demonstration of a multicomponent LIDAR and the remote composition analysis of aerosols. Because these filaments are conducting (7, 8), they have applicability in the field of lightning research.

Filamentation

Filamentation occurs when adequate high-power fs laser pulses propagate across transparent media such as glass or air (2–4, 9, 10). It is initiated by Kerr-lens self-focusing due to an intensity-dependent refractive index of matter: $n = n_0 + \Delta n_{\text{Kerr}}(I) = n_0 + n_2 I$, where $n_2 = 3 \times 10^{-19} \text{ cm}^2/\text{W}$ in air. As a consequence of the usually Gaussian transverse intensity distribution I in the laser beam, the refractive-index profile behaves like a focusing lens. When the beam power exceeds the critical power $P_{\text{crit}} = (1.22 \cdot \lambda)^2 / 128 n_2$ of several GW in air (11), the Kerr lens overcomes diffraction and leads to a beam collapse, with all the energy concentrated close to the axis. This strong focusing combined with the high power of femtosecond pulses yields high intensities, leading to high-order multiphoton ionization of air. The resulting free-electron density of 10^{16} to 10^{17} cm^{-3} contributes negatively to the index of refraction and has the effect of creating a defocusing plasma lens. From this point, the Kerr and plasma contributions to the refractive index balance out, resulting in a dynamic guiding of the light as thin filaments with a typical diameter of $100 \mu\text{m}$. The filaments propagate over distances of hundreds of meters, exceeding the Rayleigh length by orders of magnitude (12–15). The high intensity in the filaments ($\sim 4 \times 10^{13}$ to $6 \times 10^{13} \text{ W/cm}^2$) (16, 17) induces strong self-phase modulation, leading to the emission of a broadband white-light continuum ranging from 230 nm to $4.5 \mu\text{m}$ (18, 19).

A certain amount of this white light is emitted in a narrow cone in the forward direction, with a typical cone half-angle of 0.1° , ranging from longer wavelengths in the center to shorter wavelengths at the cone edges (3, 20). However, it has been shown in

the laboratory that a considerable portion of the white light is scattered preferentially in the backward direction (21). This phenomenon is of particular importance for LIDAR applications. For powers much larger than the critical power, the modulational instability breaks the beam into several filaments. Hence, the beam propagates as a bundle of parallel filaments, which vanish and reappear in new patterns over long distances (7, 22).

tion, which allows focal lengths of some hundred meters at best, and at the cost of focusing optics such as large-aperture telescopes with adaptive optics.

However, using filamentation requires control of group velocity dispersion (GVD), which normally increases the duration of short laser pulses propagating across the atmosphere. This duration increase is due to their intrinsic pulse bandwidth of typically 20

nm and occurs because the spectral components with longer wavelengths (“red” components) of the laser spectrum propagate faster than those with shorter wavelengths (“blue”). This effect, however, can be turned into an advantage by launching negatively chirped pulses, for which the blue component precedes its red component at the output of the fs-laser compressor. Such a negatively chirped pulse shortens temporally while propagating, and its intensity increases until the conditions for filamentation, which generates the white light, are reached (6).

The chirp-based control of the white-light supercontinuum has been demonstrated by using the Teramobile laser placed near the 2-m telescope of the Thüringer Landessternwarte Tautenburg (TLS) observatory in Germany. The laser beam was launched vertically, and the backscattered light was imaged through the telescope. Figure 1A shows a typical image obtained at the fundamental wavelength (800 nm) of the laser. Multiple scattering halos are observed on two haze layers at altitudes of 4 and 9 km, and the beam is visible up to more than 20 km in altitude. Tuning the same observation to the white-light continuum in the blue-green band (385 to 485 nm) and comparing images taken with different initial chirp settings (Fig. 1, B and C) shows that the white-light signal can

only be observed with adequate GVD precompensation. In Fig. 1D, the image of the conical emission of the filament appears projected on a haze layer.

The Teramobile

Field experiments require mobility to perform investigations at adequate locations. Studies of high-power fs-laser beam propaga-

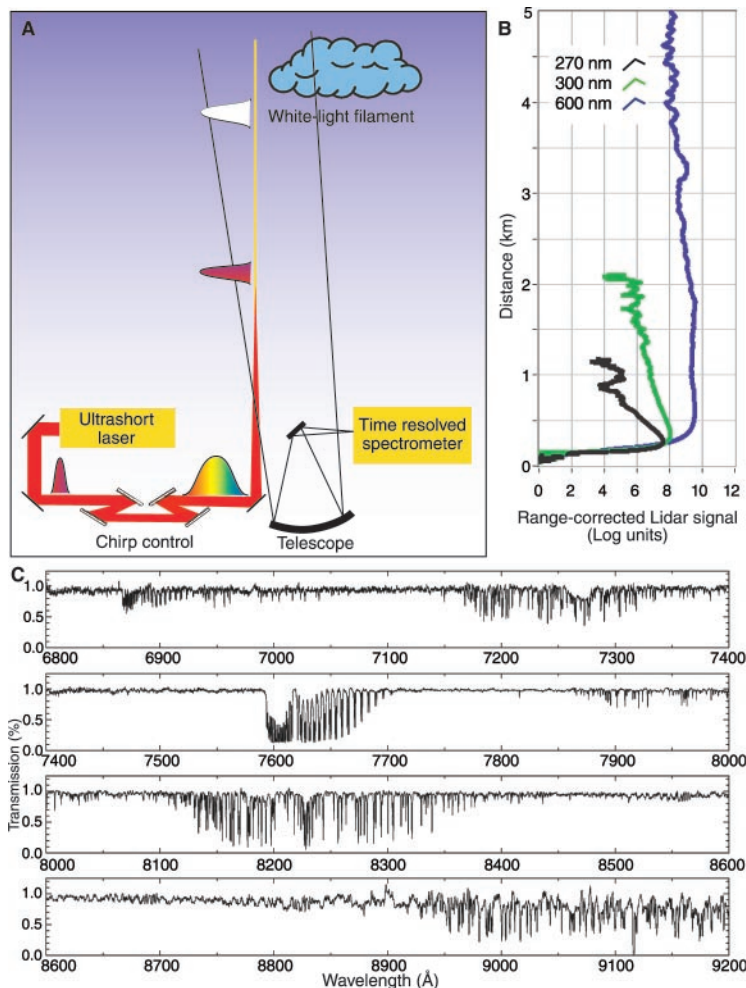


Fig. 2. White-light LIDAR. (A) Schematic of the LIDAR experimental setup. Before launch into the atmosphere, the pulse is given a chirp, which counteracts GVD during its propagation in air. Hence, the pulse recombines temporally at a predetermined altitude, where white-light continuum is produced, and then is backscattered and detected by LIDAR. (B) Vertical white-light LIDAR profile at three wavelengths: 270 nm (third harmonic), 300 nm, and 600 nm. (C) High-resolution atmospheric absorption spectrum from an altitude of 4.5 km measured in a LIDAR configuration.

Atmospheric Experiments

Atmospheric diagnostics based on nonlinear optical processes like white-light generation, multiphoton-induced fluorescence, or harmonic generation require the delivery of high laser intensities at remote distances and high altitudes. Because filamentation counteracts diffraction over long distances, it is better suited to that purpose than is linear propaga-

tion over km-range distances can only be performed realistically in outdoor experiments. The fs-LIDAR measurements have to be performed where relevant gaseous or aerosol pollutants occur, for example, in urban areas or at industrial sites. Laser-lightning studies require spots where the lightning probability is high, as well as test experiments at high-voltage facilities. These considerations clearly define the need for a mobile fs-TW laser system embedded in a standard freight container-integrated laboratory equipped with the necessary LIDAR detection, power and cooling supplies, temperature stabilization, vibration control, and an additional standard LIDAR system to ensure eye safety.

These requirements were achieved by the Teramobile system (23). The laser itself is based on the chirped-pulse amplification technique (24), with a Ti:sapphire oscillator and a Nd-yttrium aluminum garnet (YAG)-pumped Ti:sapphire amplification chain. It provides 350-mJ pulses with a 70-fs duration, resulting in a peak power of 5 TW at a wavelength of ~ 800 nm and a repetition rate of 10 Hz. Its integration in the reduced space of the mobile laboratory required a particularly compact design. The classic compressor setup has been improved into a chirp generator to precompensate the GVD in air. Combined with an adjustable focus, this setup permits us to control the distance of the onset of filamentation and its length. The LIDAR detection chain is based on a 40-cm receiving telescope, a high-resolution spectrometer equipped with a set of gratings, and detectors allowing simultaneous temporal and spectral analysis of the return signal in a wavelength range between 190 nm and 2.5 μm .

LIDAR

The principle of standard LIDAR systems is based on the effect of optical scattering of emitted light on atmospheric constituents. The Rayleigh-, Raman-, fluorescence, or Mie-scatter processes at a distance R all return a small portion of the emitted light back to the observer. This necessarily leads to an unfavorable $1/R^2$ dependency of the received light. Arc lamp-based LIDAR experiments have shown previously that the spectrally dispersed signal on the receiver is usually too weak to allow identification of atmospheric trace substances. The same question must be raised for the fs-LIDAR measurements as well because of the broad spectrum of the white-light supercontinuum. However, the strong backward component of the supercontinuum (21) opens the opportunity to establish a directional, white-light source in the atmosphere, radiating predominantly in the backward direction.

The fs-LIDAR experimental setup is shown in Fig. 2A. After passing a (negative) chirp generator, the fs-laser pulses are launched into the atmosphere. As a result, filaments are generated at a predetermined distance. The backscattered white light is then collected by a telescope and focused through a spectrometer on a time-resolved detector. Figure 2B shows three transients of spectrally filtered return signals recorded in the time window after the laser was fired: two, as an indicator for white light, were recorded at $\lambda = 300$ and 600 nm; the other was recorded at the third-harmonic (TH) wavelength ($\lambda = 270$ nm) (25). The vertical axis indicates the altitude at which the signals were backscattered. The initial strong signal increase is due to the progressive overlap between laser and telescope field of view. The white-light signal at 600 nm reaches an altitude of >5 km. Stronger Rayleigh scattering at shorter wavelengths causes the UV wavelengths to vanish shortly above 1 km. The strong decrease of the TH signal is due to a high tropospheric ozone concentration (typically 100 $\mu\text{g}/\text{m}^3$) at the time of measurement.

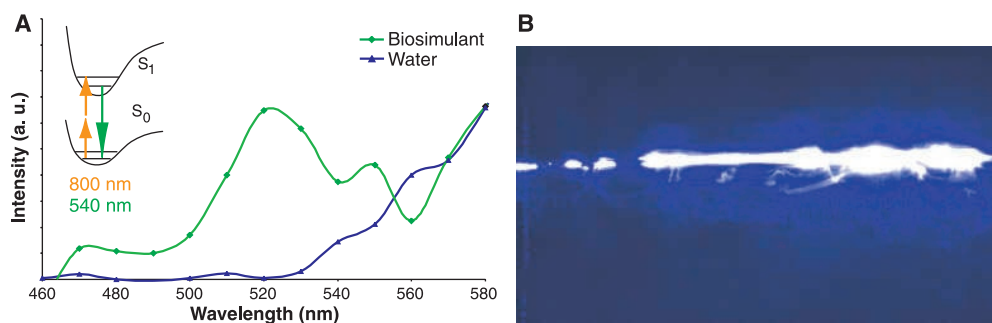


Fig. 3. Analysis (A) and synthesis (B) of aerosols with ultrashort laser. (A) LIDAR signal of the two-photon excited fluorescence from a biosimulant (riboflavin-doped water droplets) at a 50-m distance. (B) Laser-induced nucleation of water droplets in a cloud chamber. Nucleated aerosols are visible as a bright line over several tens of cm along the laser beam because they scatter light from the subsequent laser pulses.

The ability to perform high-resolution measurements over a wide spectral range using white-light LIDAR is illustrated in Fig. 2C. The measurement was recorded at an altitude of 4.5 km; it presents the highly resolved optical fingerprints of the atmosphere along this very long absorption path, allowing us to record extremely weak lines. The richness of the apparent atmospheric absorption lines represents, for example, extended ro-vibrational progressions of highly forbidden transitions of O_2 (with cross sections in the range of 10^{-25} to 10^{-24} cm^2). Simulations based on the high-resolution transmission (HITRAN) molecular absorption database of the water lines yield almost perfect agreement with the measured result (6). The experimental data also reveal lines that are not tabulated in the database. The achievable resolution sug-

gests the possibility of retrieving even humidity and temperature profiles. The use of white-light LIDAR has been demonstrated in the UV, where extended sequences of tropospheric-ozone profiles have been deduced from multispectral measurements, as well as in the infrared, where higher conversion efficiencies have been observed (26). White-light LIDAR might also simultaneously yield wind profiles through the measurement of Doppler shifts.

Aerosols

Aerosols are a key component of atmospheric pollution. They can act, for example, as catalysts for heterogeneous chemistry or as carriers for adsorbed carcinogenic species into the lungs. More recently, the prospect of bioterrorist attacks has increased the urgency for an early-warning system based on selective remote sensing of aerosols. The strong scattering by atmospheric aerosols allows ready LIDAR observation. However, their diversity of size, shape, and composition makes their remote identification a difficult challenge. Using multispectral LIDAR techniques (27), we can retrieve the abundance, particle size, and refractive index, but at

present this can only be done with aerosol models. No remote-sensing method yet allows us to determine the composition of aerosols. The high peak power of the fs pulses offers the possibility of achieving this goal by generating nonlinear effects directly inside the aerosol particles. Ultrashort pulses are focused onto a bright hot spot inside a liquid droplet as it forms a spherical microcavity. At this location, the cross section for nonlinear processes like multiphoton-excited fluorescence (MPEF) is enhanced (28). Although this fluorescence light is emitted isotropically from the hot spot, the reciprocity principle ensures that it is refocused into the backward direction by the droplet itself, favoring its detection by LIDAR. Moreover, signal optimization by pulse shaping would yield unique shaping signatures for individual fluorophores (29). This signature could allow us

REVIEW

to identify species despite their similar fluorescence spectra.

We recently applied the MPEF process to the remote identification of clean and contaminated water particles (30). In the experiment, we produced a controlled distribution of water droplets of about 1.5 μm diameter in an open cloud chamber, which was placed 50 m away from the Teramobile system. The droplets were doped with the biosimulant riboflavin, which exhibits a characteristic fluorescence emission around 540 nm. When the cloud was illuminated with adequate peak power (250 GW), a two-photon excited fluorescence signal (Fig. 3A) emerged from the riboflavin-containing droplets, allowing us to unambiguously identify the signature of the biosimulant. This result demonstrates the ability of nonlinear LIDAR to distinguish bioaerosols from natural background aerosols of the same size (Fig. 3A).

The ionized laser-induced filaments also provide the opportunity to detect supersaturation of the atmosphere directly. Supersaturation refers to an atmosphere in which water vapor has not condensed to form clouds, despite thermodynamic conditions (humidity, temperature, and pressure) that imply condensation at equilibrium. Condensation requires sufficient nucleation germs, either natural or artificial, for example, heavy molecules such as AgI. Charges induced by laser filaments—instead of the commonly used ionizing radiation from a radioactive source—can serve as nucleation germs. In our experiments, we sent fs-laser pulses into a fog chamber, allowing the supersaturated water vapor to nucleate around the radiation-induced charges. Strong droplet formation was observed inside the chamber after each laser shot (Fig. 3B). This result demonstrates the possibility of creating laser-induced nucleation germs at distances that can be controlled by the laser chirp. The ability to determine by remote probing whether the atmosphere is supersaturated is of great importance for the prediction of rain, hail, or snow.

Toward Lightning Control

The possibility of triggering and guiding lightning with laser beams has been debated for more than 30 years (31). The main concern is to protect sensitive sites, such as electrical installations or airports, from direct strikes and electromagnetic perturbations. Early studies in the 1970s and 1980s with nanosecond lasers (32) showed severe limitations arising from the lack of connected plasma channels. However, the advent of high-power fs lasers, which produce ionized plasma channels with electron densities several orders greater than that required for lightning initiation in the atmosphere, $N_{\text{init}} \approx$

$5 \times 10^{11} \text{ cm}^{-3}$ (33), opened new opportunities in this domain (34).

Rodriguez *et al.* recently demonstrated simultaneous triggering and guiding of large gap discharges in air by laser filaments (35). The Teramobile system was placed inside the high-voltage (HV) facility of the Technical University of Berlin, with its horizontal output beam in line with the electrodes. The filament spanned the whole 1- to 3-m gap between the electrodes (Fig. 4A). Figure 4B shows a typical erratic discharge between the two electrodes when no laser filament is present. Once the filaments are properly located and timed with respect to the HV pulse, a fully guided straight discharge (Fig. 4C) is obtained. Moreover, the breakdown voltage is reduced by $>30\%$, demonstrating the abil-

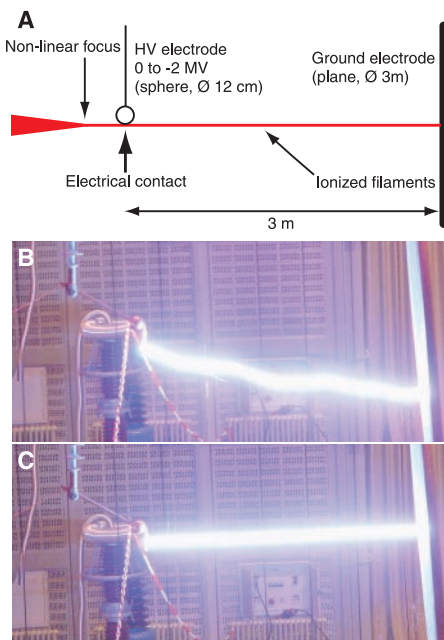


Fig. 4. Laser control of high-voltage discharges. (A) Experimental setup. (B) Free discharge over 3 m, without laser filaments. Note the erratic path. (C) Straight discharge guided along laser filaments.

ity of fs-laser filaments to trigger HV discharges by ohmic bridging of the electrodes. The experiment opens fascinating perspectives with regard to fs filament-induced triggering of lightning.

Conclusion

In the past few years, knowledge about the propagation of ultrashort laser pulses in air and the related nonlinear optical effects has progressed steadily. In particular, the extended fs laser-induced white-light filaments hold promise for applications in atmospheric science. Several encouraging experiments have raised hopes for fs laser-based lightning control and protection, as well as for remote analysis of the atmosphere in the fields of

multicomponent trace-gas diagnosis by fs white-light LIDAR, composition analysis of aerosols, and detection of atmospheric supersaturation. The development of these applications will further be assisted by the expected progress in ultrafast laser technology, such as direct diode pumping, miniaturization, and the development of two-dimensional beam profile and pulse-shaping techniques. Such innovations will greatly improve the versatility, reliability, and ease of operation of fs laser sources and hence make them even more valuable for atmospheric applications.

References and Notes

1. R. A. Meyers, Ed., *Encyclopedia of Analytical Chemistry* (Wiley, Chichester, UK, 2000), vol. 3.
2. A. Braun *et al.*, *Opt. Lett.* **20**, 73 (1995).
3. E. T. J. Nibbering *et al.*, *Opt. Lett.* **21**, 62 (1996).
4. A. L. Gaeta, *Science* **301**, 54 (2003).
5. L. Wöste *et al.*, *Laser Optoelektron.* **29**, 51 (1997).
6. P. Rairoux *et al.*, *Appl. Phys. B* **71**, 573 (2000).
7. H. Schillinger, R. Sauerbrey, *Appl. Phys. B* **68**, 753 (1999).
8. S. Tzortzakis *et al.*, *Opt. Commun.* **181**, 123 (2000).
9. A. Brodeur *et al.*, *Opt. Lett.* **22**, 304 (1997).
10. M. Mlejnek *et al.*, *Opt. Lett.* **23**, 382 (1998).
11. Y. R. Shen, *The Principles of Nonlinear Optics* (Wiley, New York, 1984).
12. M. Mlejnek, E. M. Wright, J. V. Moloney, *Opt. Express* **4**, 223 (1999).
13. N. Aközbeek, C. M. Bowden, A. Talepbour, S. L. Chin, *Phys. Rev. E* **61**, 4540 (2000).
14. A. Couairon, S. Tzortzakis, L. Bergé, M. Franco, B. Prade, A. Mysyrowicz, *J. Opt. Soc. Am. B* **19**, 1117 (2002).
15. P. Sprangle, J. R. Peñano, B. Hafizi, *Phys. Rev. E* **66**, 046418 (2002).
16. H. R. Lange *et al.*, *Phys. Rev. Lett.* **81**, 1611 (1998).
17. J. Kasparian, R. Sauerbrey, S. L. Chin, *Appl. Phys. B* **71**, 877 (2000).
18. J. Kasparian *et al.*, *Opt. Lett.* **25**, 1397 (2000).
19. N. Aközbeek *et al.*, *Opt. Commun.* **191**, 353 (2001).
20. O. G. Kosareva, V. P. Kandidov, A. Brodeur, C. Y. Chen, S. L. Chin, *Opt. Lett.* **22**, 1332 (1997).
21. J. Yu *et al.*, *Opt. Lett.* **26**, 533 (2001).
22. M. Mlejnek, M. Kolesik, J. V. Moloney, E. M. Wright, *Phys. Rev. Lett.* **83**, 2938 (1999).
23. H. Wille *et al.*, *Eur. Phys. J. Appl. Phys.* **20**, 183 (2002).
24. D. Strickland, G. Mourou, *Opt. Commun.* **56**, 219 (1985).
25. N. Aközbeek *et al.*, *Phys. Rev. Lett.* **89**, 143901 (2002).
26. G. Méjean *et al.*, *Appl. Phys. B*, in press.
27. B. Stein *et al.*, *J. Geophys. Res.* **104**, 23983 (1999).
28. V. Boutou *et al.*, *Appl. Phys. B* **75**, 145 (2002).
29. T. Brixner, N. H. Damrauer, P. Niklaus, G. Gerber, *Nature* **414**, 57 (2001).
30. G. Méjean, J. Kasparian, S. Frey, E. Salmon, J. Yu, J.-P. Wolf, in preparation.
31. D. W. Koopman, T. D. Wilkerson, *J. Appl. Phys.* **42**, 1883 (1971).
32. M. Miki, Y. Aihara, T. Shindo, *J. Phys. D: Appl. Phys.* **26**, 1244 (1993).
33. X. M. Zhao, J.-C. Diels, C. Y. Wang, J. M. Elizondo, *IEEE J. Quantum Electron.* **31**, 599 (1995).
34. H. Pépin *et al.*, *Phys. Plasmas* **8**, 2532 (2001).
35. M. Rodriguez *et al.*, *Opt. Lett.* **27**, 772 (2002).
36. The Teramobile project is funded by the Centre National de la Recherche Scientifique (France) and the Deutsche Forschungsgemeinschaft (Germany). We thank C. Bréchnignac for discussions. We are grateful to the Humboldt Foundation (A.M.) and the Institut Universitaire de France (J.-P. W.) for financial support. The team at the Thüringer Landessternwarte Tautenburg helped with vertical imaging experiments. We acknowledge support by the technical staffs in Berlin, Jena, and Lyon, and in particular by M. Barbaire, M. Kerleroux, M. Kregielski, M. Néri, F. Ronneberger, and W. Ziegler. The Teramobile Web site is at www.teramobile.org.